Supplemental Figures

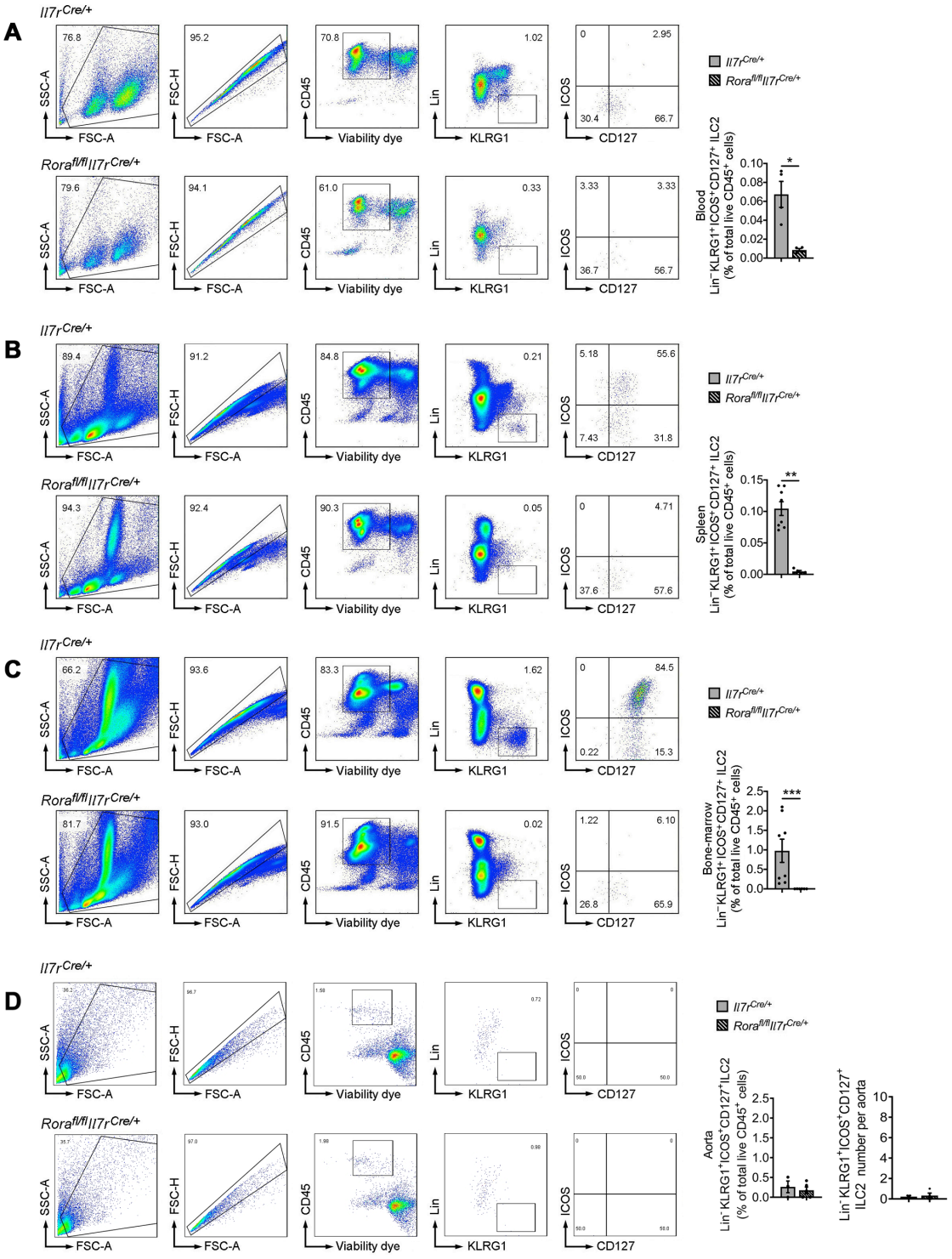

Figure S1. FACS analysis of Lin⁻KLRG1⁺ICOS⁺CD127⁺ ILC2 in blood (**A**), spleen (**B**), bone-marrow (**C**), and abdominal aorta (**D**) from *Il7r*$^{Cre/+}$ (n=4~8) and *Rora*$^{fl/fl}$*Il7r*$^{Cre/+}$ mice (n=4~8) without AAA. Data are mean±SEM. **P*<0.05, ***P*<0.01, ****P*<0.001, non-parametric Mann-Whitney *U* test.

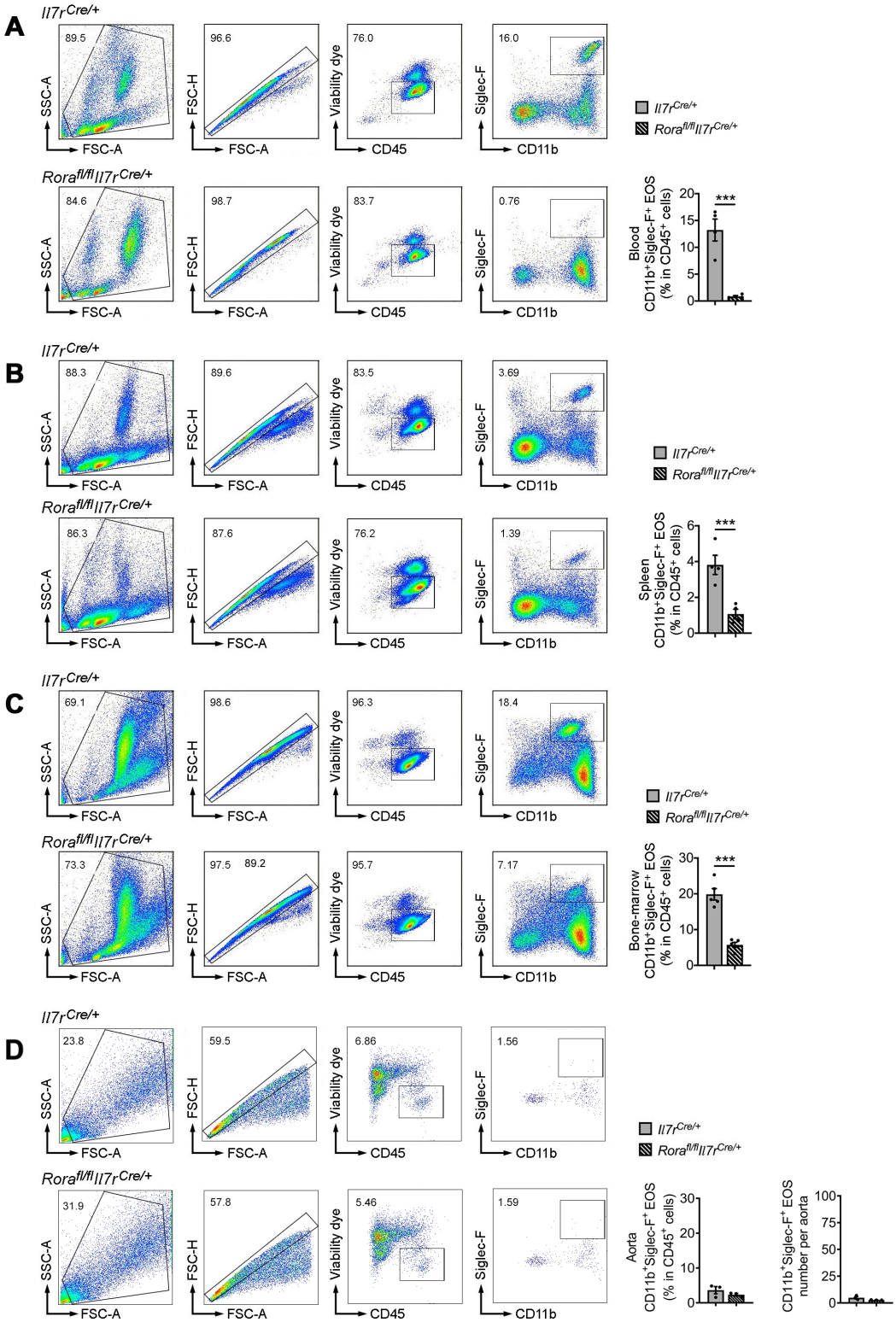

Figure S2. FACS analysis of CD11b^{+}Siglec-F^{+} EOS in blood (**A**), spleen (**B**), bone-marrow (**C**), and abdominal aorta (**D**) from *Il7r*$^{Cre/+}$ (n=4~5) and *Rora*$^{fl/fl}$*Il7r*$^{Cre/+}$ mice (n=4~5) without AAA. Data are mean±SEM. ***P<0.001, non-parametric Mann-Whitney U test.

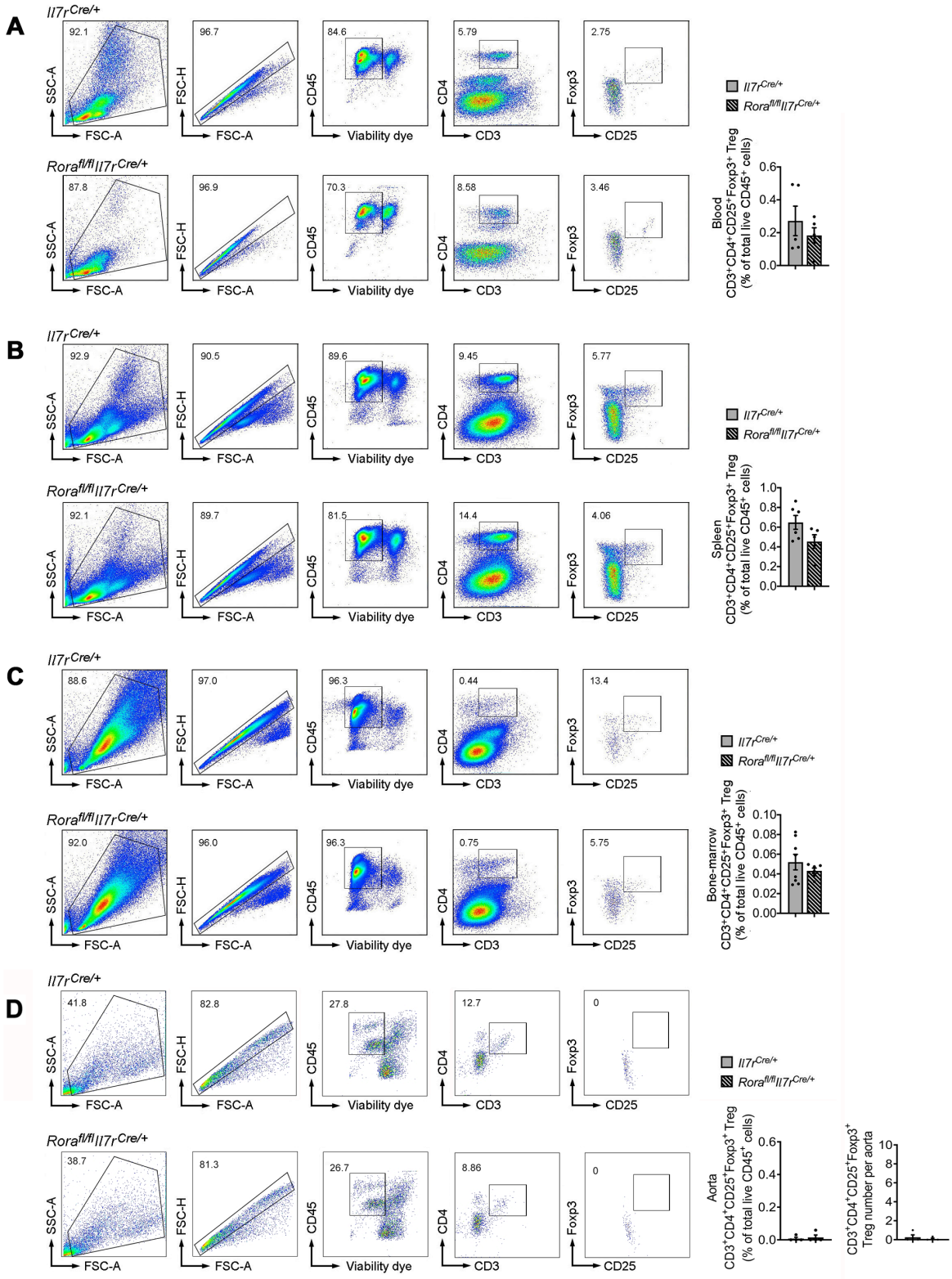

Figure S3. FACS analysis of $CD3^+CD4^+CD25^+Foxp3^+$ Treg in blood (**A**), spleen (**B**), bone-marrow (**C**), and abdominal aorta (**D**) from *Il7r*$^{Cre/+}$ (n=5~8) and *Rora*$^{fl/fl}$*Il7r*$^{Cre/+}$ mice (n=5~8) without AAA. Data are mean±SEM.

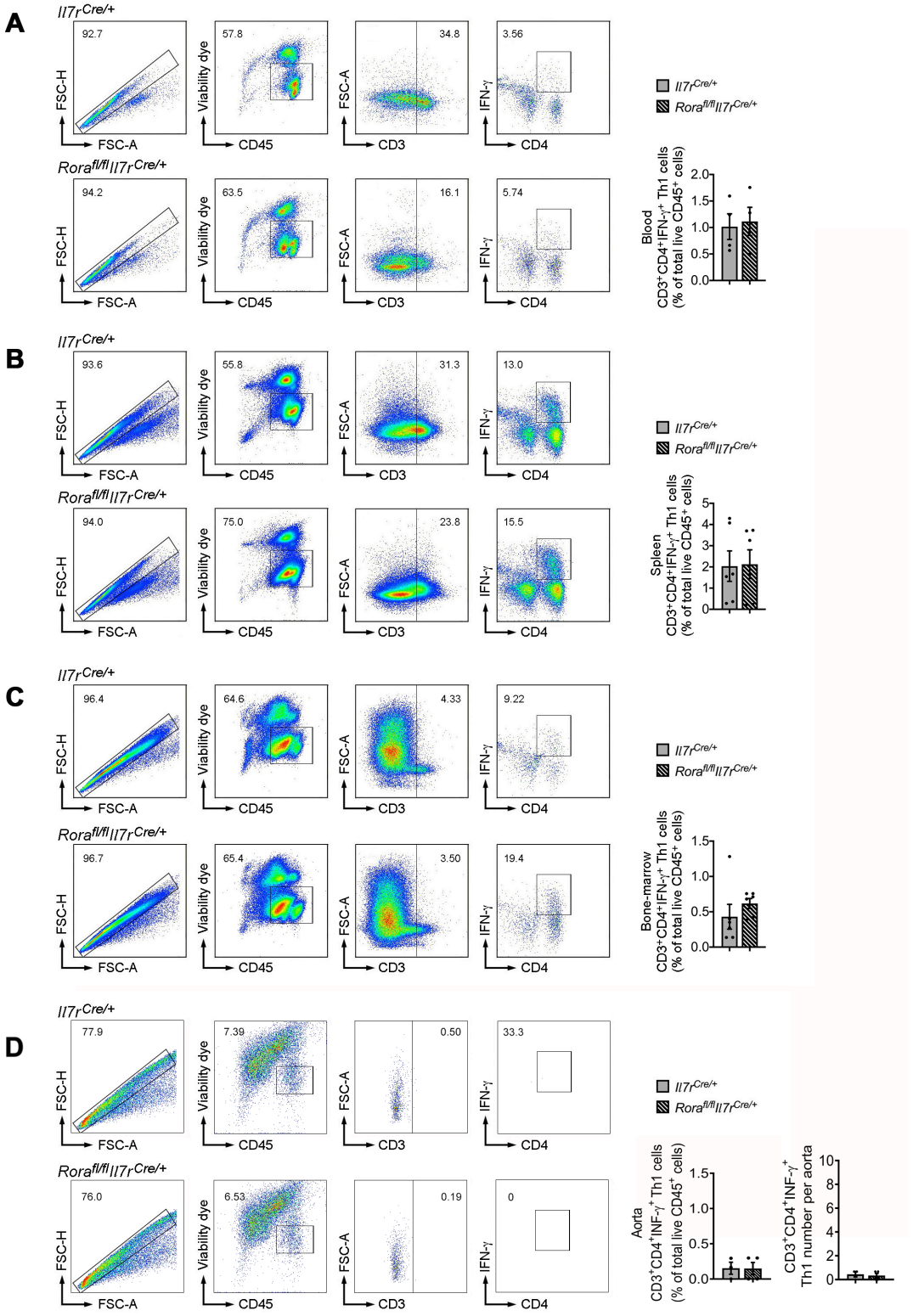

Figure S4. FACS analysis of $CD3^+CD4^+IFN\text{-}\gamma^+$ Th1 T cells in blood (**A**), spleen (**B**), bone-marrow (**C**), and abdominal aorta (**D**) from *Il7r*$^{Cre/+}$ (n=4~6) and *Rora*$^{fl/fl}$*Il7r*$^{Cre/+}$ mice (n=4~6) without AAA. Data are mean±SEM.

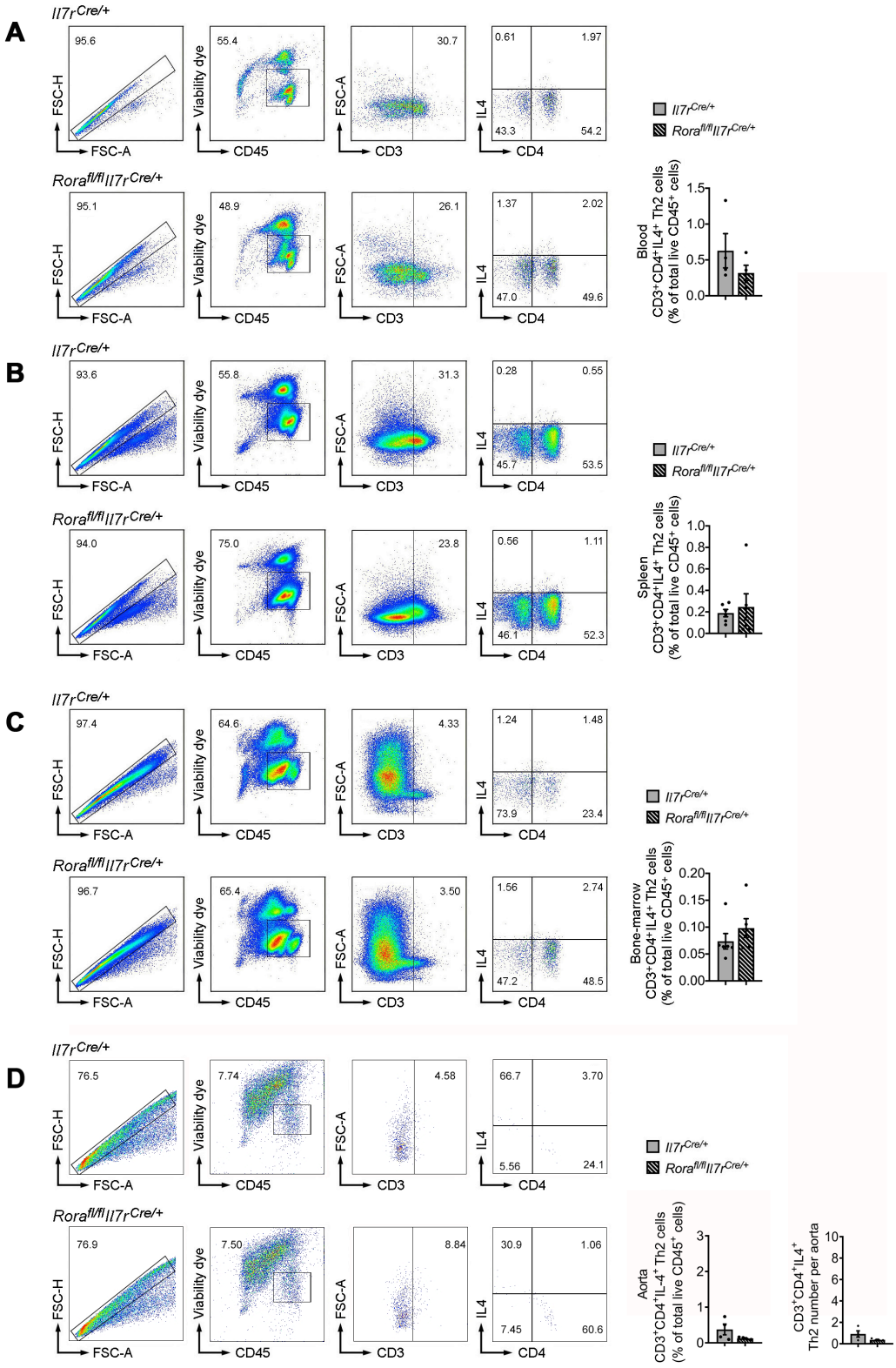

Figure S5. FACS analysis of $CD3^+CD4^+IL4^+$ Th2 T cells in blood (**A**), spleen (**B**), bone-marrow (**C**), and abdominal aorta (**D**) from *Il7r*$^{Cre/+}$ (n=4~6) and *Rora*$^{fl/fl}$*Il7r*$^{Cre/+}$ mice (n=4~6) without AAA. Data are mean±SEM.

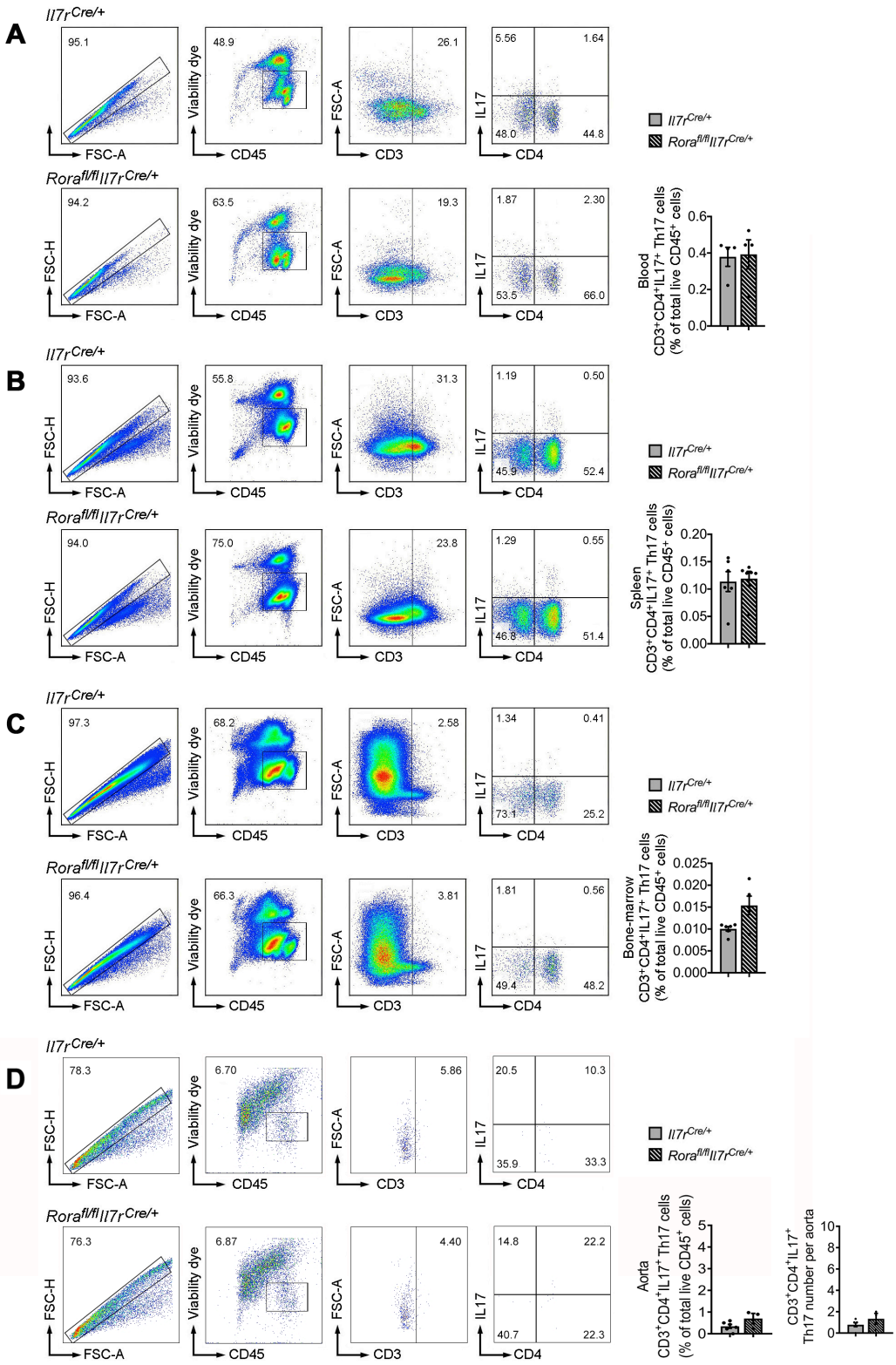

Figure S6. FACS analysis of $CD3^+CD4^+IL17^+$ Th17 T cells in blood (**A**), spleen (**B**), bone-marrow (**C**), and abdominal aorta (**D**) from $Il7r^{Cre/+}$ (n=4~6) and $Rora^{fl/fl}Il7r^{Cre/+}$ mice (n=4~6) without AAA. Data are mean±SEM.

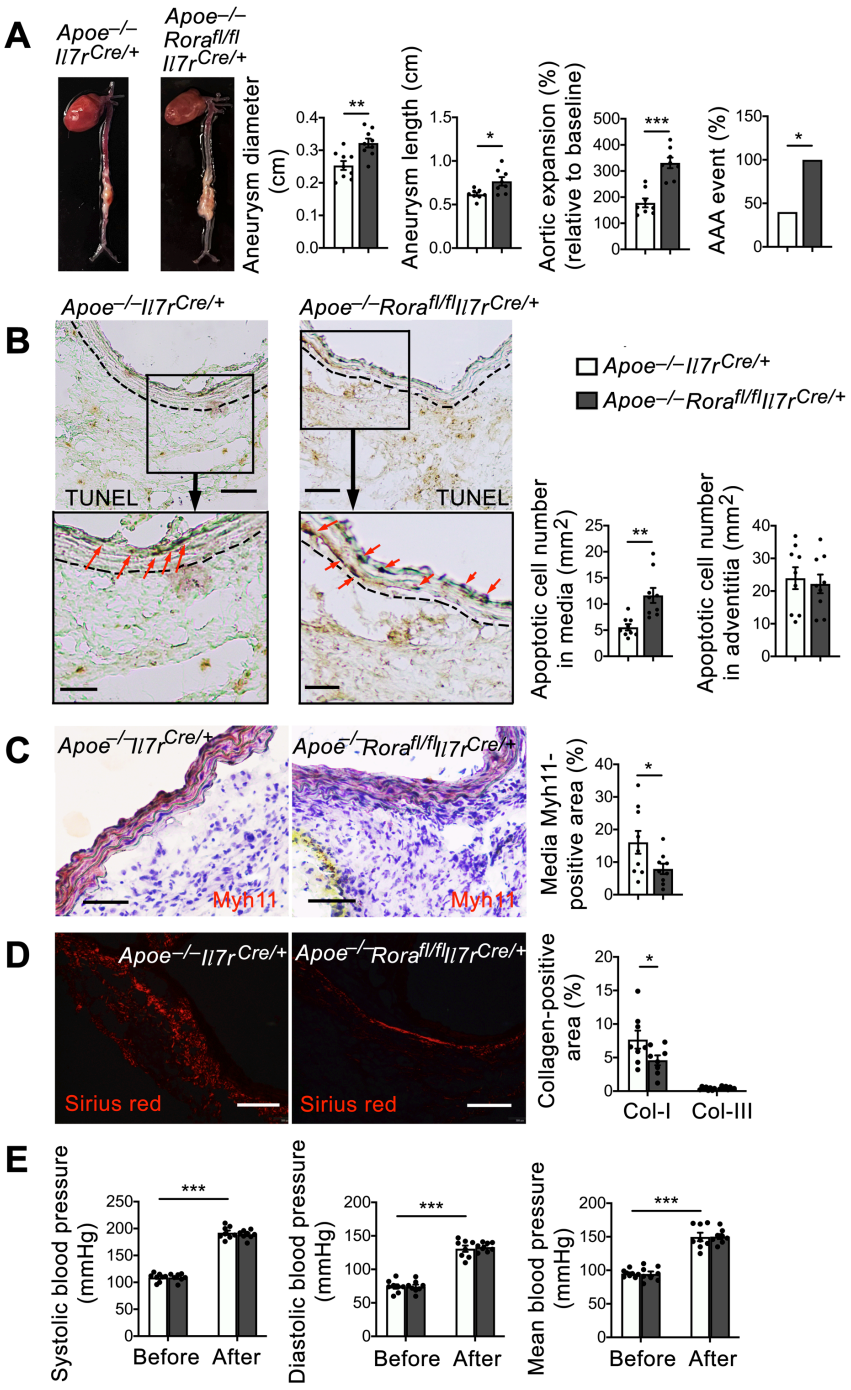

Figure S7. Characterization of Ang-II perfusion-induced AAA at 28 days after surgery. Both *Apoe*$^{-/-}$*Il7r*$^{Cre/+}$ (n=8) and *Apoe*$^{-/-}$*Rora*$^{fl/fl}$*Il7r*$^{Cre/+}$ mice (n=8) underwent Ang-II perfusion-induced AAA production. **A.** AAA diameter and representative images on the left, power: 0.916, AAA lesion length, Aortic diameter expansion percentage relative to the baseline (before surgery), and AAA incidence rate as defined by diameter increase by 150% or higher. **B.** TUNEL staining and media and adventitia apoptotic cell contents. **C.** Media Myh11-positive SMC area in AAA lesions. **D.** Collagen-I and –III area in AAA lesions. **E.** Blood pressures before and after AAA. Data are mean±SEM, ***P*<0.01, ****P*<0.001, non-parametric Mann-Whitney *U* test.

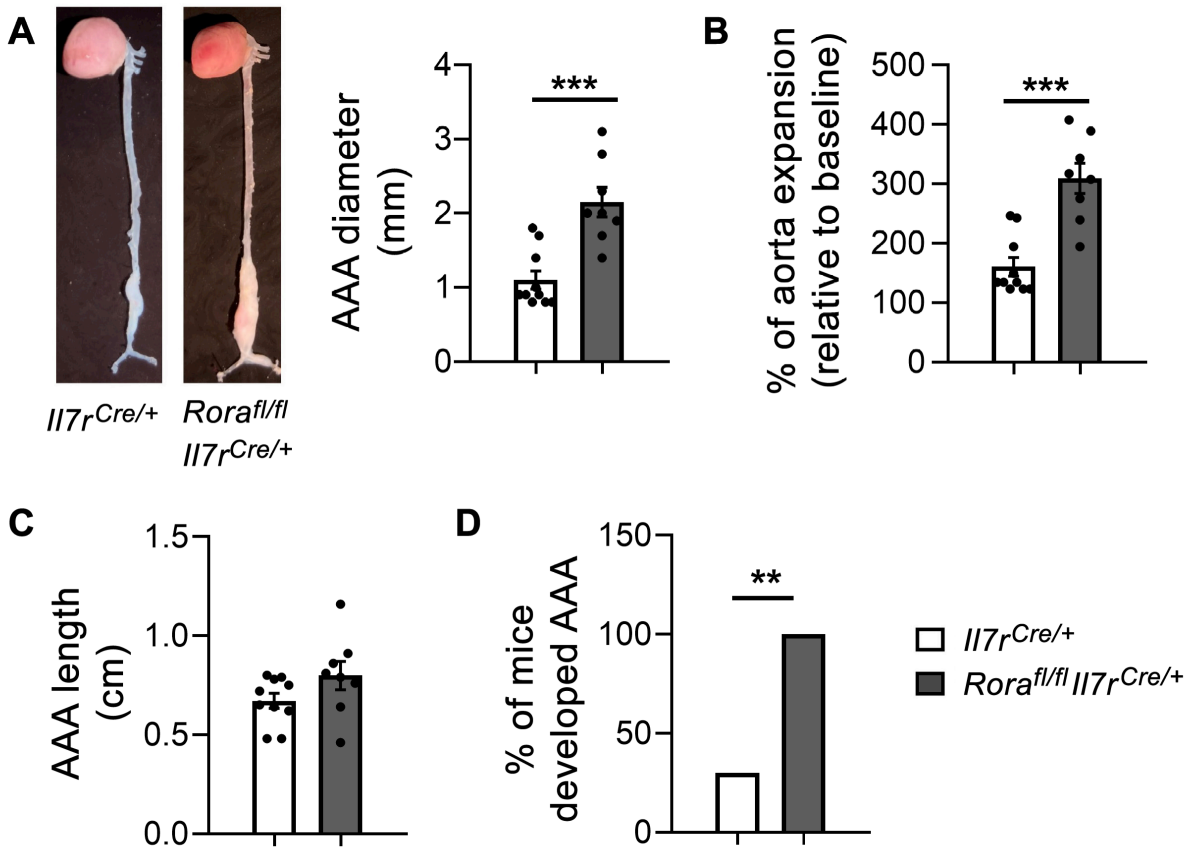

Figure S8. Characterization of peri-aortic elastase injury-induced AAA at 28 days after the injury. Both *Il7r*$^{Cre/+}$ (n=10) and *Rora*$^{fl/fl}$*Il7r*$^{Cre/+}$ mice (n=8) underwent peri-aortic elastase injury-induced AAA production. **A.** AAA diameter and representative images on the left. Power: 0.951. **B.** Aortic diameter expansion percentage relative to the baseline (before surgery). Power: 0.915. **C.** AAA lesion length. **D.** AAA incidence rate as defined by diameter increase by 150% or higher. Data are mean±SEM, ***P*<0.01, ****P*<0.001, non-parametric Mann-Whitney *U* test (**A-C**) and Fisher's exact test (**D**).

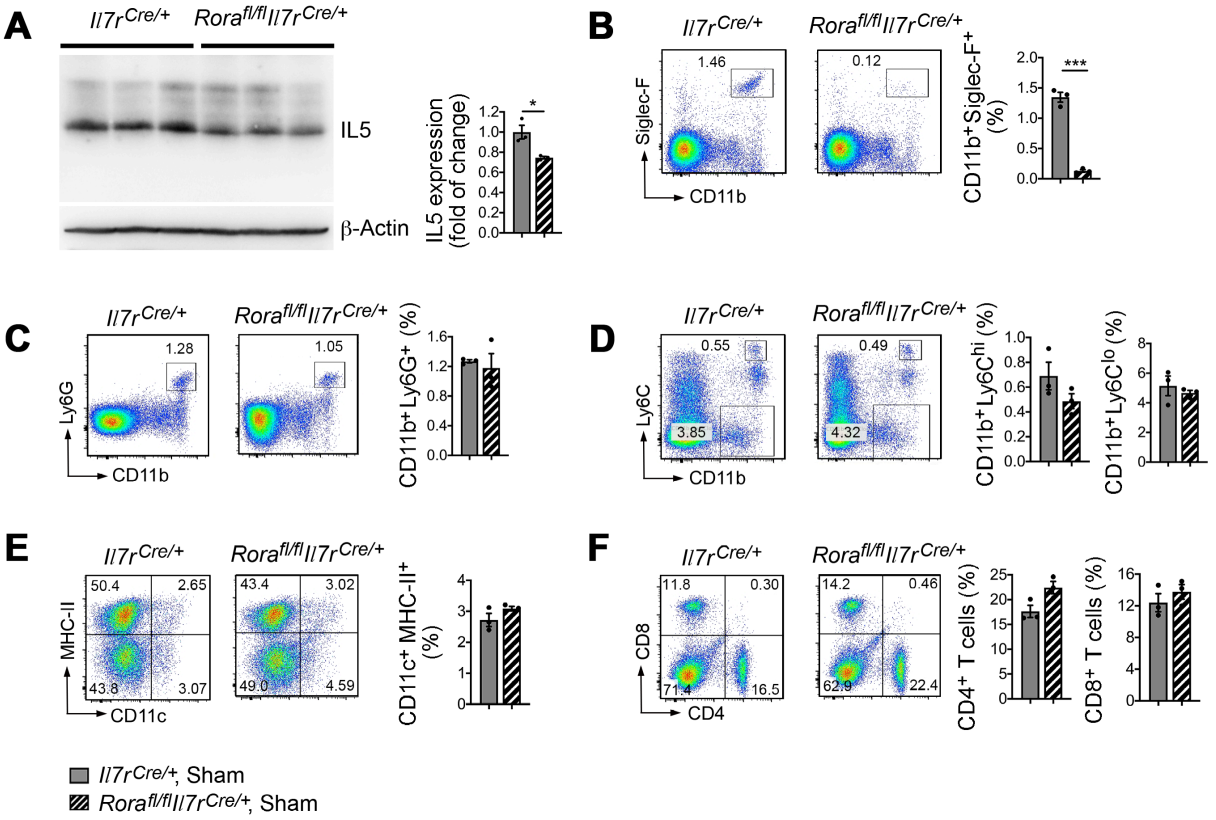

Figure S9. ILC2 deficiency reduces bone-marrow IL5 expression and spleen EOS contents in *Rora*$^{fl/fl}$*Il7r*$^{Cre/+}$ mice without AAA. **A.** Immunoblot analysis of IL5 in bone-marrow preparations from *Il7r*$^{Cre/+}$ and *Rora*$^{fl/fl}$*Il7r*$^{Cre/+}$ mice without AAA. n=3 each. **B-F.** FACS analysis of splenic CD11b^{+}Siglec-F^{+} EOS (**B**), CD11b^{+}Ly6G^{+} neutrophils (**C**), CD11b^{+}Ly6C^{hi} and CD11b^{+}Ly6C^{lo} monocytes (**D**), CD11c^{+}MHC-II^{+} DCs (**E**), and CD4^{+}CD8^{-} and CD4^{-}CD8^{+} T cells (**F**) from *Il7r*$^{Cre/+}$ and *Rora*$^{fl/fl}$*Il7r*$^{Cre/+}$ mice before AAA formation. Data are mean±SEM. n=3 per group. **P*<0.05, ****P*<0.001, non-parametric Mann-Whitney *U* test.

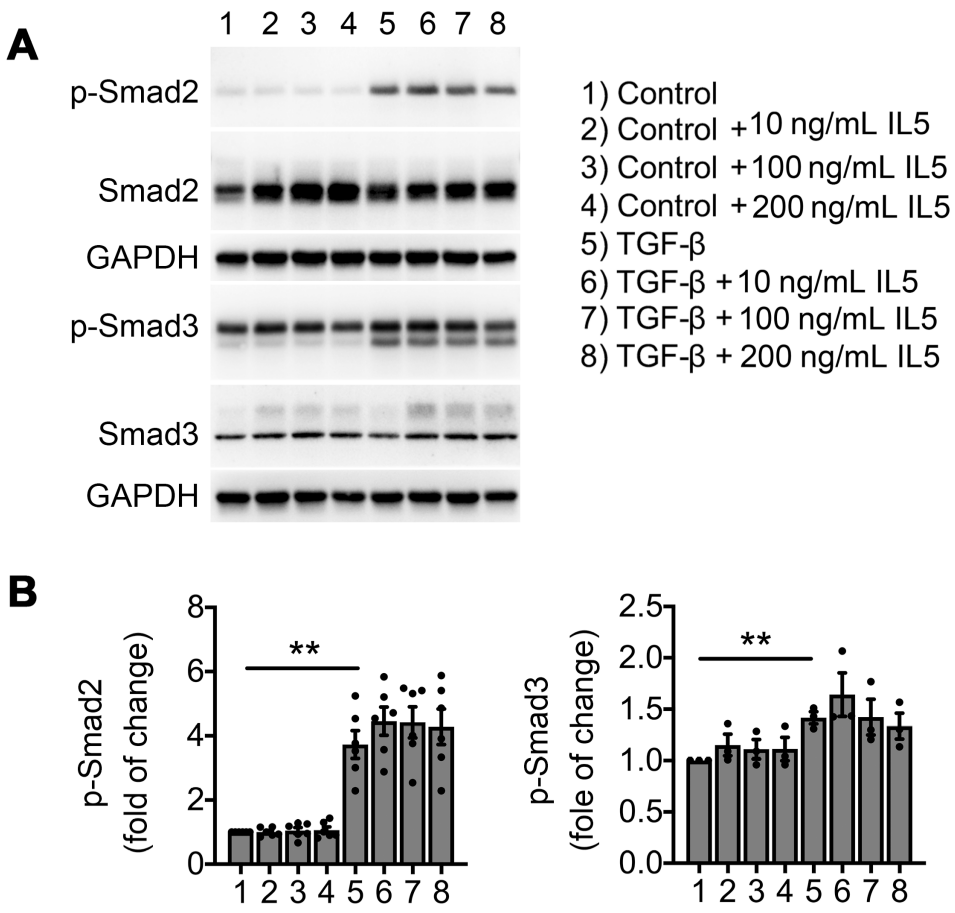

Figure S10. IL5 does not affect TGF-β-induced aortic SMC Smad2/3 signaling. Immunoblots (**A**) and quantification (**B**) of p-Smad2 and p-Smad3 from cultured aortic SMCs treated with or without TGF-β and different concentrations of IL5 as indicated. Data are mean±SEM. n=3~6 per group. ***P*<0.01, one-way ANOVA test.

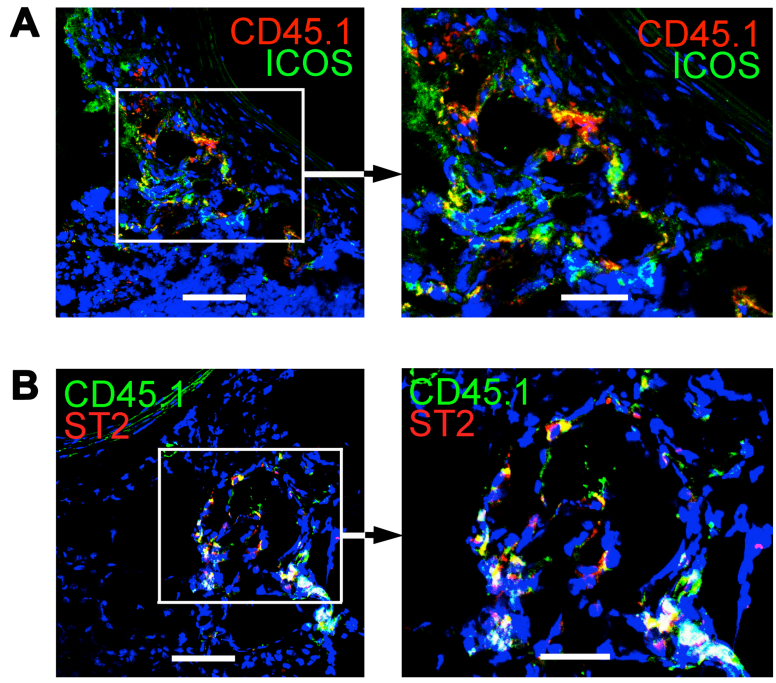

Figure S11. Immunofluorescent staining of AAA lesions from *Rora*$^{fl/fl}$*Il7r*$^{Cre/+}$ recipient mice received donor CD45.1^{+} ILC2. **A.** Donor CD45.1^{+} ILC2 expression of ICOS. **B.** Donor CD45.1^{+} ILC2 expression of ST2.

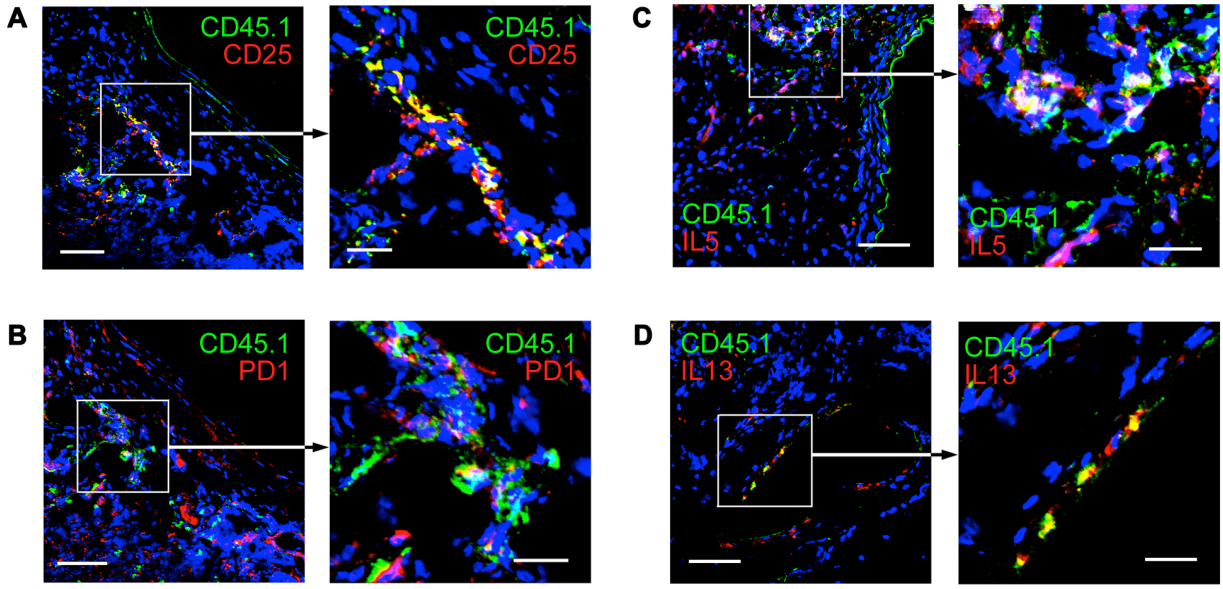

Figure S12. Immunofluorescent staining of AAA lesions from *Rora*$^{fl/fl}$*Il7r*$^{Cre/+}$ recipient mice received donor CD45.1^{+} ILC2. **A.** Donor CD45.1^{+} ILC2 expression of CD25. **B.** Donor CD45.1^{+} ILC2 expression of PD1. **C.** Donor CD45.1^{+} ILC2 expression of IL5. **D.** Donor CD45.1^{+} ILC2 expression of IL13.

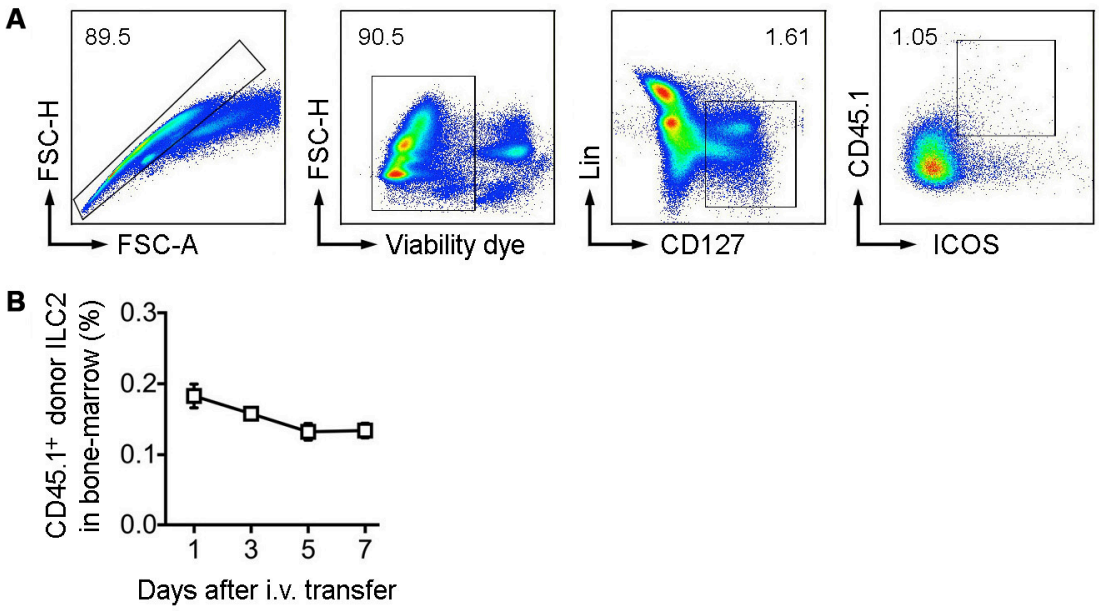

Figure S13. FACS analysis of bone-marrow $Lin^{-}CD127^{+}ICOS^{+}CD45.1^{+}$ donor ILC2 in *Rora*$^{fl/fl}$*Il7r*$^{Cre/+}$ recipient mice at 1, 3, 5, and 7 days after donor cell i.v. transfer and peri-aortic $CaPO_4$ injury-induced AAA. **A.** FACS gating strategy. **B.** Bone-marrow ILC2 contents. N=4 per data point.

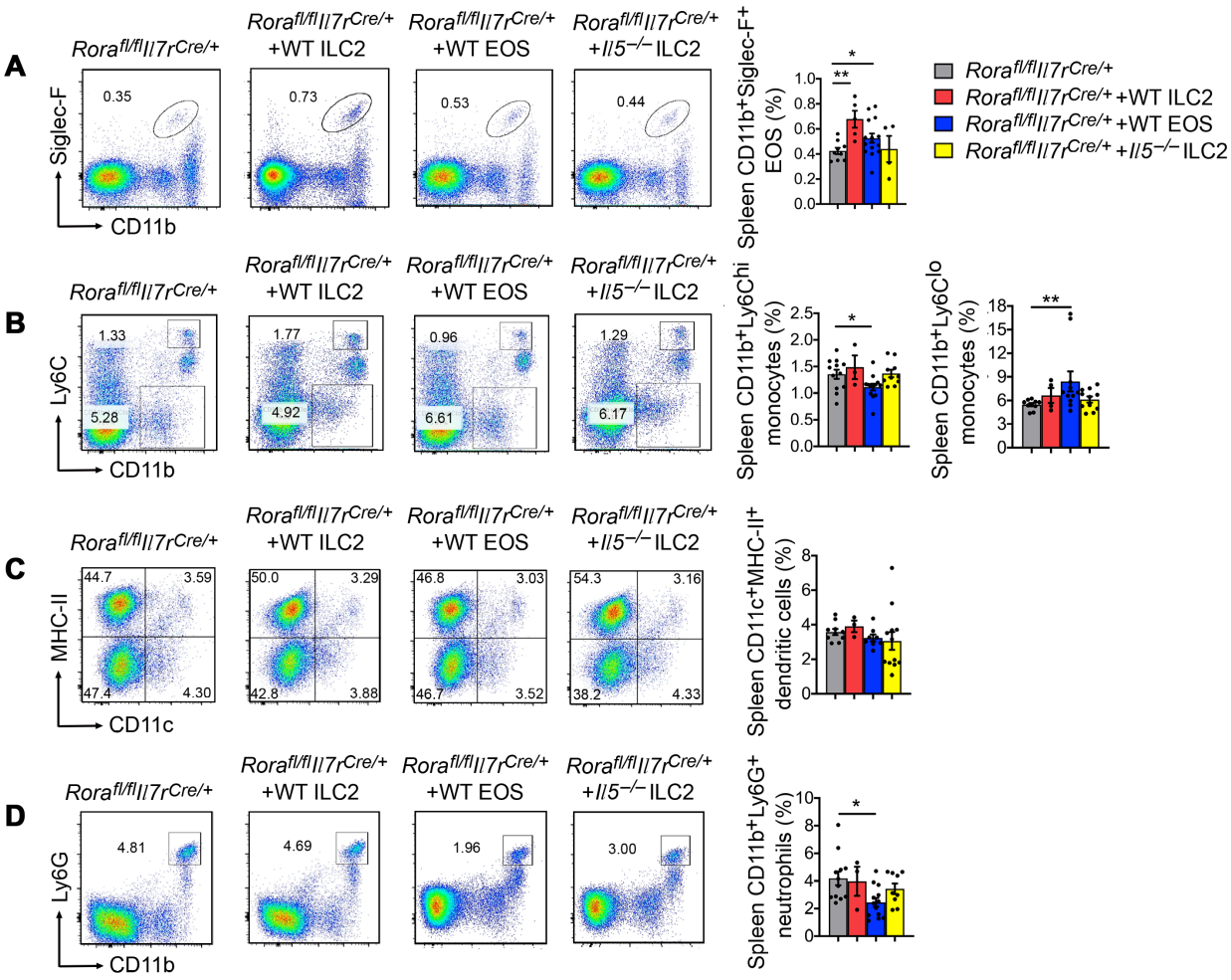

Figure S14. FACS analysis of splenic CD11b^{+}Siglec-F^{+} EOS (**A**), CD11b^{+}Ly6C^{hi} and CD11b^{+}Ly6C^{lo} monocytes (**B**), CD11c^{+}MHC-II^{+} dendritic cells (**C**), and CD11b^{+}Ly6G^{+} neutrophils (**D**) from *Rora*$^{fl/fl}$*Il7r*^{Cre} mice reconstituted with or without EOS from WT mice or ILC2 from WT or *Il5*$^{-/-}$ mice. Representative FACS images are shown to the left. Data are mean±SEM. n=3~15 mice per group. **P*<0.05, ***P*<0.01, one-way ANOVA test.

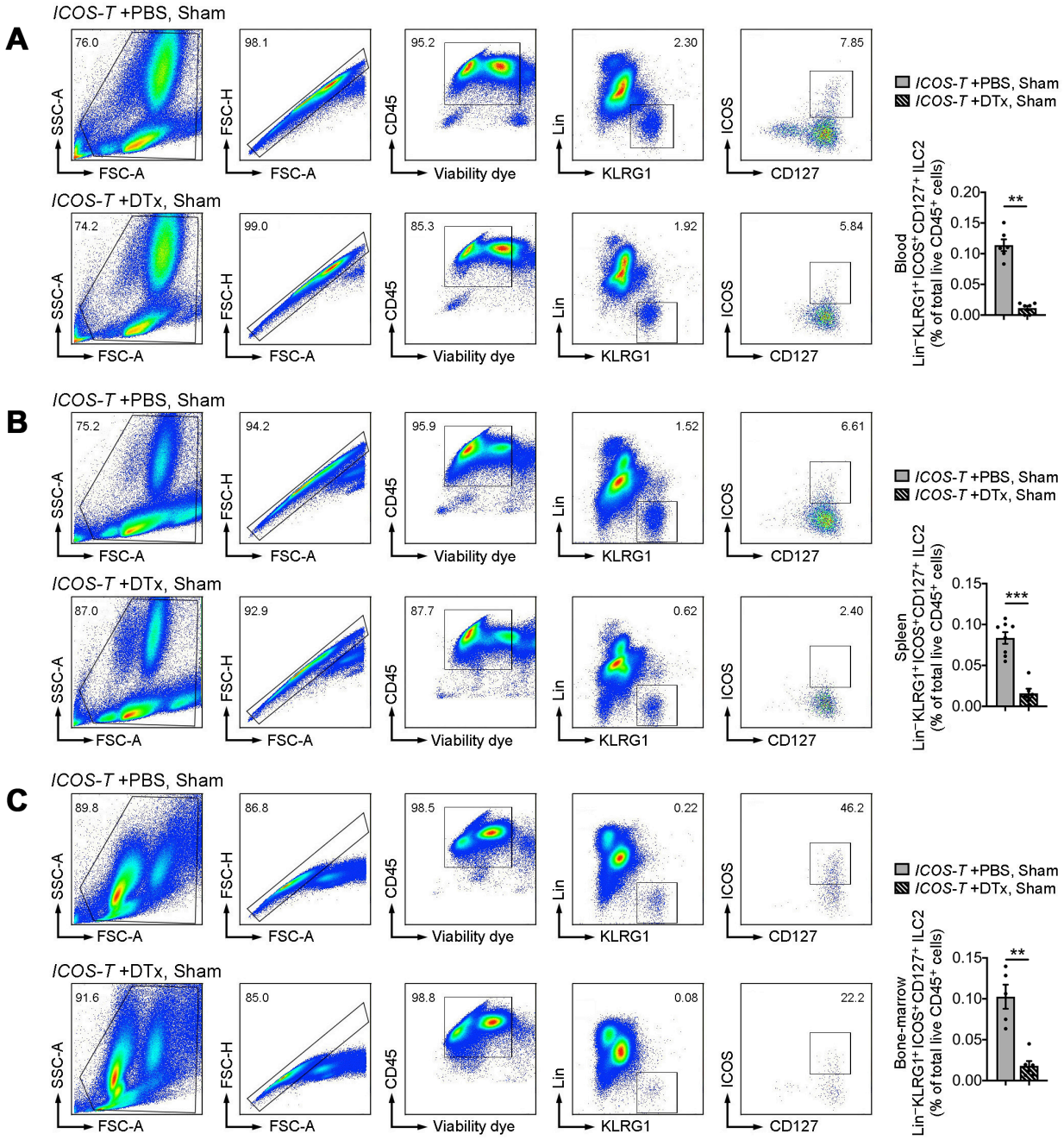

Figure S15. FACS analysis of Lin$^-$KLRG1$^+$ICOS$^+$CD127$^+$ ILC2. *ICOS-T* mice received PBS (n=5~8) or DTx (n=6) for 5 days, followed by FASC analysis of Lin$^-$KLRG1$^+$ICOS$^+$CD127$^+$ ILC2 in peripheral blood (**A**), spleen (**B**), and bone-marrow (**C**) in these mice without AAA production. ***P*<0.01, ****P*<0.001, non-parametric Mann-Whitney *U* test.

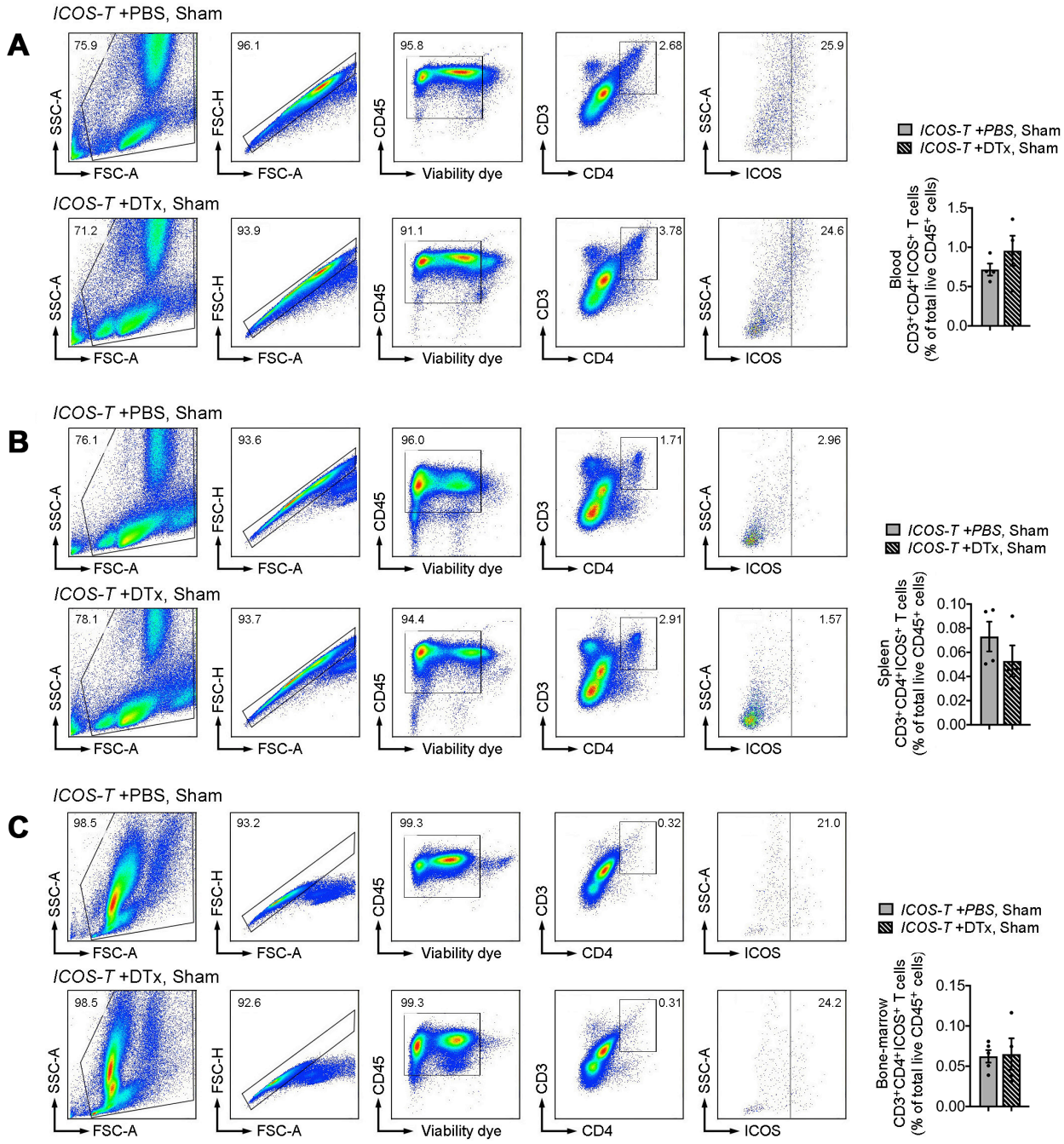

Figure S16. FACS analysis of $CD3^+CD4^+ICOS^+$ T cells. *ICOS-T* mice received PBS (n=4~5) or DTx (n=4) for 5 days, followed by FASC analysis of $CD3^+CD4^+ICOS^+$ T cells in peripheral blood (**A**), spleen (**B**), and bone-marrow (**C**) in these mice without AAA production.

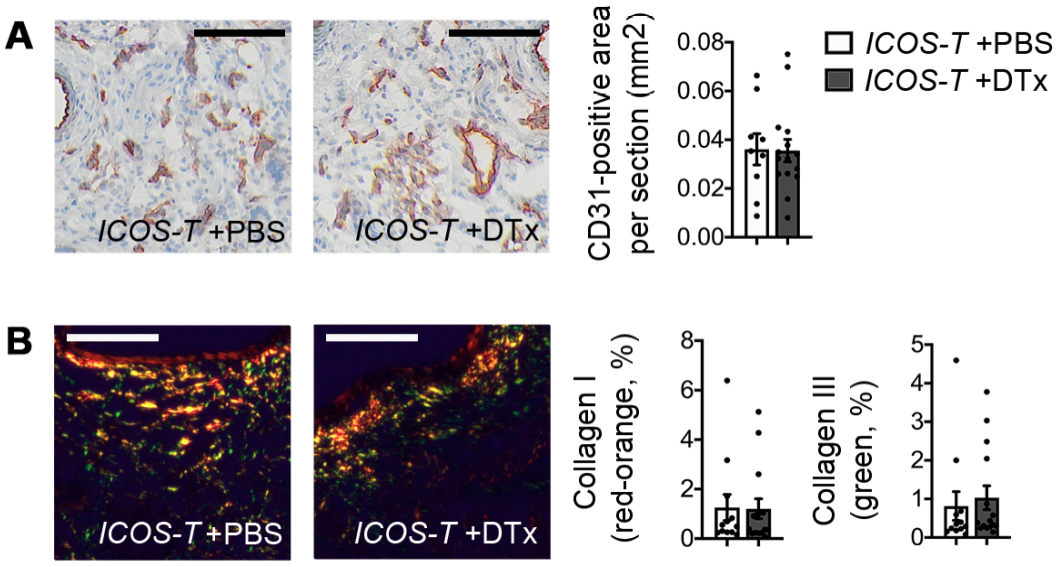

Figure S17. Induced ILC2 depletion did not affect AAA lesion angiogenesis or collagen deposition. **A.** Immunostaining detected CD31-positive microvessel areas in AAA lesions from *ICOS-T* mice treated with PBS or DTx. Scale: 50 μm. **B**. Sirius red staining of AAA lesions from *ICOS-T* mice treated with PBS or DTx. Scale: 50 μm. Data are mean±SEM. n=12 and 15 mice per group. Non-parametric Mann-Whitney *U* test was used.

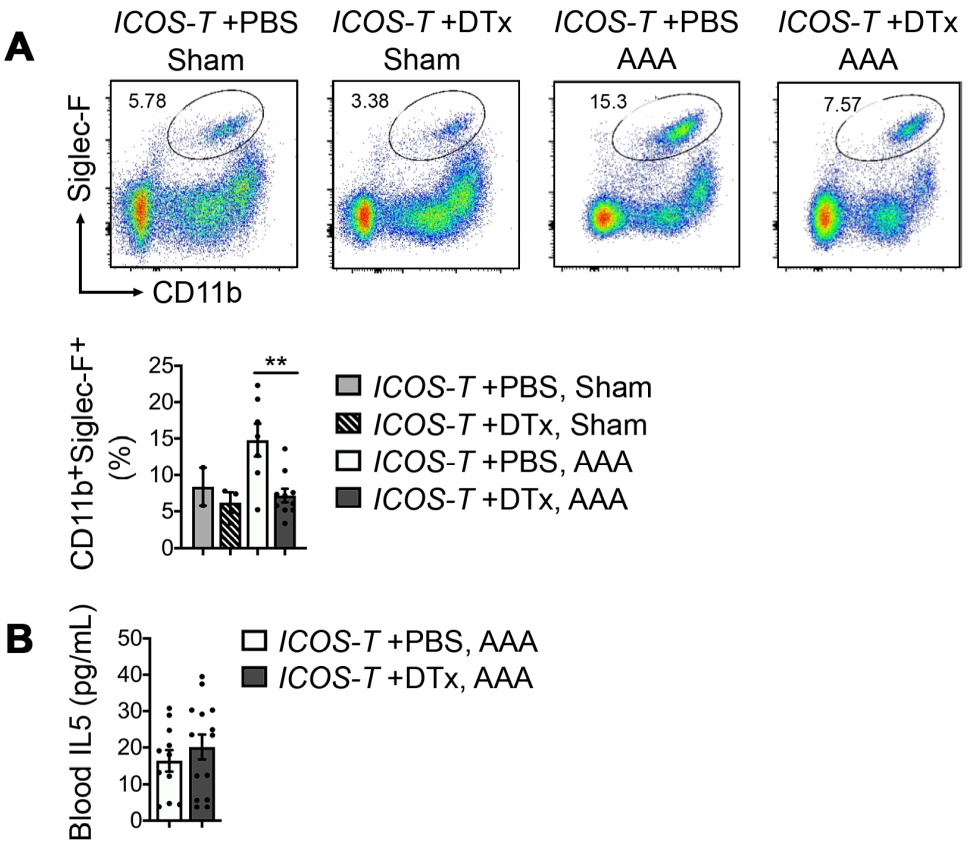

Figure S18. Splenic EOS and blood IL5 in *ICOS-T* mice treated with PBS or DTx. **A.** FACS analysis of splenic CD11b^{+}Siglec-F^{+} EOS in *ICOS-T* mice treated with PBS or DTx. Representative FACS images were shown to the top. Data are mean±SEM. n=3~10 mice per group. ***P*<0.01, one-way ANOVA test. **B**. Blood IL5 levels in *ICOS-T* mice treated with PBS or DTx. Data are mean±SEM. n=11~14 mice per group. Non-parametric Mann-Whitney *U* test was used.